Irreversibility Analysis of Magneto-Micropolar Fluid Flow Past an Inclined Stretchable Sheet with Viscous Dissipation

[1]Fatunmbi, E.O. & [2]Are, S.O
[1-2]Department of Mathematics and Statistics
Federal Polytechnic
Ilaro, Nigeria.
E-mail: [1]ephesus.fatunmbi@federalpolyilaro.edu.ng, [2]stephen.are@federalpolyilaro.edu.ng

ABSTRACT

This article numerically investigates irreversibility analysis on the flow of an electrically conducting micropolar fluid configured in an inclined nonlinear stretchable sheet. The model under investigation couples the influences of viscous dissipation, non-uniform viscosity and heat source, suction/injection velocity and power law thermal boundary condition. The approach of similarity transformations is applied to transform the governing equations into ordinary differential equations and then numerically solved using shooting techniques alongside Runge-Kutta algorithms. Graphical solutions of the effects of the various controlling physical parameters are depicted and deliberated appropriately. Besides, the accuracy of the numerical code used is checked with related published studies under limiting conditions and found to be strongly correlated. The investigation reveals that heat transfer irreversibility overrides that of viscous dissipation and magnetic field with an uplift in the radiation parameter while the opposite occurs with a rise in the material parameter. More so, the velocity and entropy generation profiles enlarged with advancement in the the material micropolar parameter.

Keywords: Irreversibility analysis; Micropolar fluid; Viscous dissipation; Non-uniform heat source

25th iSTEAMS Trans-Atlantic Multidisciplinary Conference Proceedings Reference Format
Fatunmbi, E.O. & Are, S.O (2020): Irreversibility Analysis of Magneto-Micropolar Fluid Flow Past an Inclined Stretchable Sheet with Viscous Dissipation. Proceedings of the 25th iSTEAMS Trans-Atlantic Multidisciplinary Virtual Conference, Laboratoire Jean Kuntzmann, Universite Laboratoire Jean Kuntzmann, Universite Grenoble, Alpes, France June – July, 2020. Pp 155-168 www.isteams.net/France2020.

1. INTRODUCTION

The flow of non-Newtonian fluids depart markedly from that of Newtonian fluids. A nonlinear relationship exists between the shear rate and shear stress in the Non-Newtonian fluids, also these fluids typically display shear thinning or thickening attributes and sometimes yield stress. In view of the complexity in the nature of these fluids, the equations of the flow are highly nonlinear in nature. However, due to unquantifiable and unparalleled applications derivable from these fluids in science, technology, engineering and industries, various researchers and scientists have devoted time and energy to investigate them. The application of these fluids are found in oil drilling processes, food processing, coating and polymers operations, mud drilling, pharmaceuticals, cosmetics and so on (Hayat et al, 2013; Dalair et al., 2014; Gholinia et al., 2018). There are various models of non-Newtonian fluids which have been formulated due to the differences that exist in the the rheological features of fluids which make it impossible to capture all the characteristics of the non-Newtonian fluids in one model..

These models include: the micropolar fluid, Casson fluid, Maxwell fluid, tangent hyperbolic fluid, Jeffery, Ostwald De-Wald power law fluid, Giesekus fluid to mention a few (Sha et al., 2020; Fatunmbi & Okoya, 2020). Micropolar fluid is notable among others due to its intrinsic ability to capture and describe fluids with microstructure. The concept of the micropolar fluids explains fluids with rigid bar-like or spherical particles with the attribute of rotation and translation. This concept is suitable for simulating complex and complicated fluids with rigid, bar-like particles. Fluids that describe the micropolar fluids are liquid crystal, suspension solutions, colloids, polymeric fluids, animal blood and so on (Lukazewick, 1999).. Eringen (1966, 1972) conceptualize the micropolar fluid concept and its extension to thermo-micropolar fluid. The engineering applications of such fluids are encountered in the bio-mechanic and chemical engineering, extrusion of polymer, slurry technologies, synovial lubrication, arterial blood flows, knee cap mechanics, etc (Reena and Rana, 2009).

In high temperature situations, the assumption of uniform fluid properties cannot be valid because a rise in temperature compels the fluid transport phenomena to improve owing to a reduction in the viscosity. In such cases, the hydrodynamic and thermal boundary layer as well as the rate of heat transfer at the sheet are affected. Hence, it is imperative to investigate the influence of temperature-dependent viscosity for a realistic prediction. Such concept is applicable in engineering and industrial processes including, wire drawing, hot rolling, food processing, paper and textile production (Akinbobola and Okoya, 2015, Parida *et al.,* 2015).. Makinde (2012) applied numerical technique to discuss the impact of variable viscosity on a the flow of reactive Newtonian fluid with convective surface condition while Fatunmbi and Okoya (2020) studied such phenomenon on the flow of micropolar fluid and Khan et al. (2018) applied viscosity variation to study the flow of Powell-Eyring fluid passing an inclined sheet.

The investigation of entropy generation analysis of flow and heat transfer in thermal engineering systems is significant for the identification of the factors which promote the decay of the available energy. This energy decay can affect the efficient performance of the thermal devices. Hence, the understanding of the entropy production minimization in thermal engineering systems such as air separators, reactors, chillers and fuel cells is indispensable for the design of suitable thermal appliances. In heat transfer problems, entropy generation is a means of measuring the irreversibility that takes place in a system with the use of the second law of thermodynamics. The entropy generation measures the level of the work destruction that is available in a system, hence,, it becomes necessary to find out the rate of entropy generation in a system with an intent of upgrading such system. Besides, investigation of irreversibility analysis reveals various sources energy destruction in a system and at such, those sources which contribute to entropy can be identified and possibly reduce in order to achieve an optimal energy required in a system. The idea of irreversibility analysis was developed by Bejan (1982; 1986) who investigated heat transfer and thermal design using thermodynamics second law.

Due to crucial application of such concept, various researchers have examined it on different configurations, conditions and assumptions. Mondal *et al.* (2020) analyzed entropy generation in a hydromagnetic nanofluid with the dusty fluid flow with variable viscosity and radiation effect. Salawu *et al*. (2018) studied the irreversibility analysis of an electrically conducting Powell-Eyring fluid flow influenced by temperature-dependent thermal conductivity and associated with chemical reaction in a porous channel. Makinde and Eegunjobi (2018) reported on entropy analysis in a hydromagnetic fluid in porous stretching sheet whereas Salawu and Fatunmbi (2017) conducted a research using third grade fluid associated with entropy analysis in the presence of variable viscosity and convective cooling in a porous device. Seth et al. (2018) studied nanofluid flow passing a nonlinear stretched plate while Fatunmbi and Adeniyan(2020) lately engaged micropolar fluid to study such a concept.

During fabrication processes such as in polymer extrusion, the quality of the final product depends to a large extent on the rate of stretching sheet and the cooling rate. Hence, Crane (1970) initiated the flow passing a linearly stretching surfaces. The extended versions of such concept on different geometries can be found in the work of (Gupta and Gupta, 1977; Kumar, 2009; Qasim, 2013; Fatunmbi and Fenuga, 2018). Meanwhile, in practical situations, the stretching of the sheet is not always linear but nonlinear or exponential in nature (Cortell, 2007 & 2008, Fatunmbi, Okoya and Makinde, 2020; Fatunmbi and Adeniyan, 2020). Such studies find practical applications in industrial and engineering activities including, manufacturing of paper and textile, the aerodynamic extrusion of plastic sheet, glass blowing.

The aim of the present study is to investigate irreversibility analysis and heat transfer of a dissipative, magneto-micropolar fluid over an inclined stretching sheet with Joule heating, thermal radiation coupled with variable magnetic field and viscosity and power law surface temperature associated with a weak concentration of the micro-particles. A computational approach via shooting technique alongside Runge-Kutta method is engaged to integrate the dimensionless equations of the flow, heat transfer and entropy generation while the effects of the main parameters are graphically illustrated and discussed..

2. MODELLING OF THE PROBLEM

Consider a steady, two-dimensional flow of an incompressible, dissipative and electrically conducting micropolar fluid passing an inclined nonlinearly stretched permeable sheet. The corrdinate of the flow are (x, y), where $x\ axis$ is taken in the flow direction while y axis is normal to it as depicted in Fig. 1.

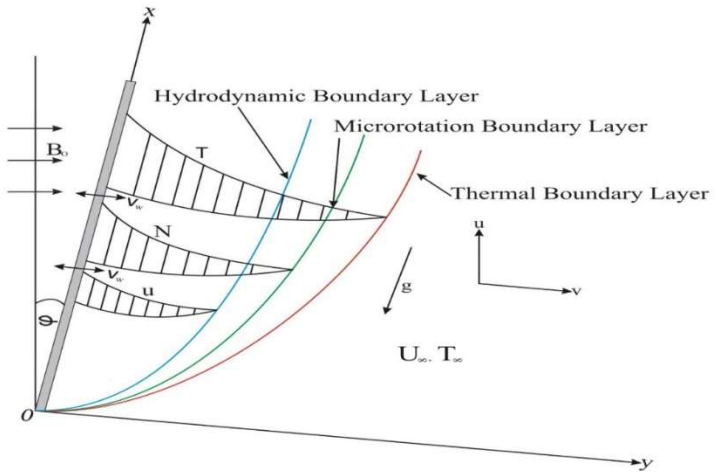

Fig. 1..The Flow Configuration

The velocity components corresponding to the directions are u and v. The fluid electrical conductivity depends on the component of velocity in the direction of x direction, i.e. $\sigma_0' = \sigma_0 u$. Similarly, a non-uniform externally applied transverse magnetic field in the direction of y is perpendicular to the flow direction. It is of strength $\mathbf{B} = (0, B(x)), B(x) = \frac{B_0}{\sqrt{x}}$ where x indicates the coordinate along the surface and B_0 denotes the strength of the

magnetic. Ignoring the induced magnetic field on the basis of significantly low Reynolds number and the electric field is also not considered..The viscosity of the fluid is taken to temperature-dependent in an inverse relationship, the heat generation or absorption is similarly assumed to be of varying type. The velocity of the sheet moves in a nonlinear nature expressed as $u = hx^n$ where $h > 0$ is a constant and n is the power law index. The case of $n = 1$ indicates a linearly stretching case.

On the basis of the aforementioned assumptios and taking into consideration the boundary layer and Oberbeck-Boussinesq approximations, the outlining equations are listed as follows

$$\frac{\partial u}{\partial x} + \frac{\partial v}{\partial y} = 0, \tag{1}$$

$$u\frac{\partial u}{\partial x} + v\frac{\partial u}{\partial y} = \frac{1}{\rho_\infty}\frac{\partial}{\partial y}\left(\mu(T)\frac{\partial u}{\partial y}\right) + \frac{R}{\rho_\infty}\frac{\partial^2 u}{\partial y^2} + \frac{\mathrm{R}}{\rho_\infty}\frac{\partial N}{\partial y} + g\beta_T(T - T_\infty)cos\alpha - \frac{\sigma_0{}'(B(x))^2}{\rho_\infty}u \tag{2}$$

$$u\frac{\partial N}{\partial x} + v\frac{\partial N}{\partial y} = \frac{\gamma}{\rho j}\frac{\partial^2 N}{\partial y^2} - \frac{R}{\rho j}\left(2\mathrm{N} + \frac{\partial u}{\partial y}\right), \tag{3}$$

$$u\frac{\partial T}{\partial x} + v\frac{\partial T}{\partial y} = \frac{k}{\rho_\infty c_p}\left(1 + \frac{16\sigma^\star T_\infty^3}{3k^\star k}\right)\frac{\partial T^2}{\partial y^2} + \frac{(\mu+R)}{\rho_\infty c_p}\left(\frac{\partial u}{\partial y}\right)^2 + \frac{\sigma_0{}'(B(x))^2}{\rho_\infty c_p}u^2 + \frac{q'''}{\rho_\infty c_p}, \tag{4}$$

The conditions at the boundary are as follows:

$$\begin{aligned} &u = u_w = cx^n, v = v_w, N = -m\frac{\partial u}{\partial y}, T = T_w = (Ax^r + T_\infty)\ at y = 0, \\ &u \longrightarrow 0, N \longrightarrow 0, T \longrightarrow T_\infty\ as\ y \to \infty. \end{aligned} \tag{5}$$

While the non-uniform heat source/sink in Eq. (4) is expressed as

$$q''' = \frac{\kappa u_w}{x^n \nu}[H^\star(T_w - T_\infty)f' + J^\star(T - T_\infty)]. \tag{6}$$

Following the previous researchers (Afridi, 2017; Fatunmbi and Adeniyan, 2020) the volumetric entropy generation for the magneto-micropolar fluid flow in the presence of thermal radiation and viscous dissipation can be expressed as

$$S_G = \frac{\kappa}{T^2}\left[(\nabla T)^2 + \frac{16\sigma^\star T_\infty^3}{3k^\star \kappa}(\nabla T)^2\right] + \frac{(\mu+R)}{T}\left(\frac{\partial u}{\partial y}\right)^2 + \frac{\sigma_0{}'(B(x))^2}{T}u^2. \tag{7}$$

Where x and y are cartesian coordinates with corresponding components of velocity expressed as u and v. Similarly, $\mu, T, T_w, T_\infty, N, k^\star, \nu, \kappa, R, j,\ c_p, \gamma, r$ and $\sigma^\star$ respectively indicates viscosity, temperature of the fluid, sheet temperature, free stream temperature, microrotation component, mean absorption coefficient, kinematic viscosity, thermal conductivity, vortex viscosity, micro-inertial density, specific heat at constant pressure, spin gradient viscosity, temperature exponent and Stefan-Boltzmann constant. Also, $H^\star = bx^{n-1}$ and $J^\star = b^\star x^{n-1}$ in Eq. (6) are the space and heat dependent source/sink respectively. The suction/injection

velocity is indicated by v_w with $v_w = V_0 x^{(n-1)/2}$ (see Ishak, 2020; Makinde, 2020) where V_0 is a constant whereas m depicts the micropolar boundary term with $0 \leq m \leq 1$.

The temperature-dependent viscosity is expressed as

$$\frac{1}{\mu} = \frac{1}{\mu_\infty}[1 + L(T - T_\infty)] = Z(T - T_r), \tag{8}$$

with

$$Z = \frac{L}{\mu_\infty}, T_b = T_\infty - \frac{1}{L}, \tag{9}$$

where L is a constant corresponding to the fluid thermal property, μ_∞ indicates the free stream fluid viscosity, Z and T_b are constants.

The similarity and the dimensionless variables in Eq. (10) are introduced to transform the governing equations to ordinary differential equations.

$$\eta = y\left[\frac{h(n+1)x^n}{2x\nu_\infty}\right]^{1/2}, \psi = x^{(n+1)/2}\left[\frac{2\nu_\infty c}{(n+1)}\right]^{1/2} f(\eta), N = x^{(3n-1)/2}\left[\frac{h^3(n+1)}{2\nu_\infty}\right]^{1/2} g(\eta)$$
$$u = \frac{\partial\psi}{\partial y} = hx^n f', v = -\frac{\partial\psi}{\partial x} = -\left[\frac{c\nu_\infty(n+1)}{2}\right]^{1/2} x^{(n-1)/2}\left(f + \frac{(n-1)}{(n+1)}\eta f'\right), \gamma = \left(\mu + \frac{R}{2}\right)j, \tag{10}$$
$$\theta(\eta) = \frac{T-T_\infty}{T_w-T_\infty} = \frac{T-T_b}{T_w-T_\infty} + \theta r, \theta r = \frac{T_b-T_\infty}{T_w-T_\infty}, j = \left(\frac{\nu}{h}\right)x^{(1-n)}.$$

$$Fw = \frac{-\sqrt{2}V_0}{\left(\sqrt{h\nu(n+1)}\right)}, M = \frac{\sigma_0 B_o^2}{\rho}, \lambda = \frac{Gr}{Re^2}, Gr = \frac{g\beta_T(T_w - T_\infty)x^3}{\nu^2}, Re = \frac{u_w x}{\nu}, Nr = \frac{16T_\infty^3\sigma^\star}{3k^\star\kappa}$$
$$\theta r = -\frac{1}{L(T_f - T_\infty)}, K = \frac{R}{\mu_\infty}, Ec = \frac{u_w^2}{cp(T_w - T_\infty)}, Pr = \frac{\mu_\infty c_p}{k^*\kappa}, \alpha = \frac{b\kappa}{\mu_\infty c_p}, \beta = \frac{b^\star\kappa}{\mu_\infty c_p}, Br = Pr.Ec.$$

Substituting the quantities in Eq.(10) into the governing equations and taking cognizance of Eqs. (8) the governing Eqs. (2-4, 7) yield the underlisted equations:

$$\left(\frac{\theta r}{\theta r-\theta} + K\right)f''' + ff'' + Kg' - \left(\frac{2}{n+1}\right)[(n+M)f'^2 - \lambda\theta\cos\varphi] + \frac{\theta r}{(\theta r-\theta)^2}\theta' f'' = 0, \tag{11}$$

$$(1 + K/2)g'' + fg' - \left(\frac{3n-1}{n+1}\right)f'g - (2g + f'')\left(\frac{2K}{n+1}\right) = 0, \tag{12}$$

$$(1 + Nr)\theta'' - \left(\frac{2r}{n+1}\right)Prf'\theta + Prf\theta' + \left(\frac{\theta r}{\theta r-\theta} + K\right)PrEcf''^2 + \left(\frac{2}{n+1}\right)PrMEcf'^3 + Pr(\alpha f' + \beta\theta)\left(\frac{2}{n+1}\right) = 0. \tag{13}$$

$$Ns = \frac{S_G}{S_c} = \frac{(1+Nr)\theta r'^2}{(\theta+\Omega)^2} + \frac{Br}{(\theta+\Omega)}\left(\frac{\theta r}{\theta r-\theta} + K\right)f''^2 + \frac{2BrM}{(\theta+\Omega)}f'^3, \tag{14}$$

The parameters in Eq. (10) include: $\theta r, K, Fw, \lambda, M, \alpha, \beta, Gr, Ec, Pr$, These are respectively described as viscosity parameter, material (micropolar) parameter, suction/injection term, buoyancy parameter, Magnetic field parameter, space-dependent source/sink, temperature-dependent heat source/sink, Grashof number, Eckert number, Prandtl number and $\Omega = T_\infty/(T_w - T_\infty)$ represents the non-dimensional temperature difference..The sources of entropy generation in Eq. (14) are the heat transfer (HTC) or the conduction effect indicated by $\frac{(1+Nr)\theta r'^2}{(\theta+\Omega)^2}$, i.e. the first term on right of Eq. (14), the viscous dissipation irreversibility $\frac{Br}{(\theta+\Omega)}\left(\frac{\theta r}{\theta r-\theta}+K\right)f''^2$ (VDI) which is the second term while the last term on the RHS of Eq. (14) is $\frac{2BrM}{(\theta+\Omega)}f'^3$ (OHI) which denotes Ohmic heating irreversibility, where Ns describes the overall entropy production in the system and $S_c = \kappa h/\nu$ represents its characteristic. More so, engineers are also interested in the significant input of each source of entropy generation in a system. The Bejan number Be $(0 \leq Be \leq 1)$ measures such a concept and it is defined as the ratio of entropy production by heat transfer to the total entropy in the system.

$$Be \quad = \frac{NH}{NH+VDI+OHI}, \tag{15}$$

Also, the boundary conditions transorm to

$$\begin{aligned} &f'(0) = 1, f(0) = Fw, g(0) = -mf'', \theta(0) = 1, \\ &f'(\infty) = 0 g(\infty) = 0, \theta(\infty) = 0. \end{aligned} \tag{16}$$

3. NUMERICAL METHOD AND ITS VALIDATION

For the solution of the dimensionless equations, a computer algebra symbolic Maple 2016 package is applied to solve Eqs. (11-15) subject to the boundary conditions Eq. (16). The numerical approach relies on the shooting techniques alongside fourth order Runge-Kutta method. From the process of the computation, the values of the skin friction coefficien $(-f''(0))$ and Nusselt number $(-\theta'(0))$ are found. In the numerical analysis, the following values are used as the default parameter values: $\theta r = 5.0, K = M = 2.0, Ec = 0.1, Gr = 4.0, M = 2.0, n = r = Nr = 0.5, Pr = 0.71, \varphi = \frac{\pi}{6}, Fw = 0.2, Ec = 0.1 = \Omega, Br = 0.2, \alpha = \beta = 0.3$. Unless otherwise listed on the graphs. The accuracy of the numerical code employed is tested by comparing the solutions obtained for the values of $(-\theta'(0))$ in the limiting scenarios with the work of Grubka and Bobba (1985) as shown in Table 1. More so, the computed values of the skin friction coeffient $(-f''(0))$ is croschecked with the report of Hayat et al (2008) as well as Lu *et al (2018)* as presented in Tables 2.

Table 1: Computational values of $(-\theta(0))$ as compared with Grubka and Bobba (1985) for variations in r and Pr for $n = 1, K = Ec = M = \alpha = \beta = Fw = 0$ and $\theta r \to \infty$

	Grubka & Bobba		Present	
r	$Pr = 0.72$	$Pr = 1.0$	$Pr = 0.72$	$Pr = 1.0$
- 2.0	0.7200	1.0000	0.72069	0.99945
- 1.0	0.0000	0.0000	-0.00110	0.00012
0.0	-0.4631	-0.5820	-0.46359	-0.58201
1.0	-0.8086	-1.0000	-0.80883	-1.00001
2.0	-1.0885	-1.3333	-1.08862	-1.33333
3.0	-1.3270	-1.6154	-1.32707	-1.61538

Table 2: Computational values of $-f''(0)$ as compared with existing studies for variation in n when $K = \lambda = Ec = M = \varphi = fw = 0$ and $\theta r \to \infty$

n	Hayat *et al.* (2008)	Lu *et al.* (2018)	Present
0.0	0.627555	0.627547	0.627563
0.2	0.766837	0.766758	0.766846
0.5	0.889544	0.889477	0.889552
1.0	1.000000	1.000000	1.000008
1.5	1.061601	1.061587	1.061609
3.0	1.148593	1.148588	1.148601

4. RESULTS ANALYSIS AND DISCUSSION

The behaviour of selected controlling physical parameters on the velocity, temperature, entropy generation and Bejan number proifles are illustrated graphically and discussed in this section..

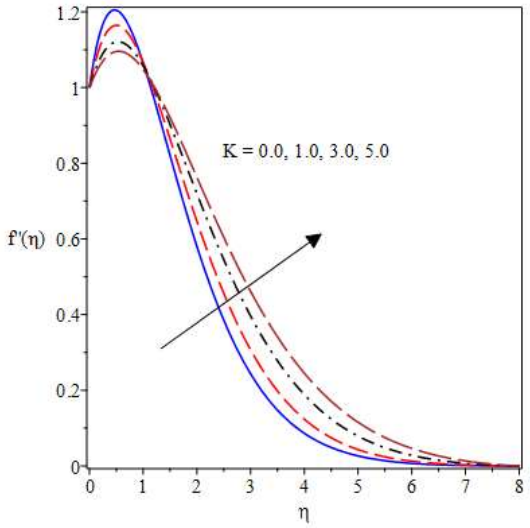

Fig. 2 Curves of velocity for K

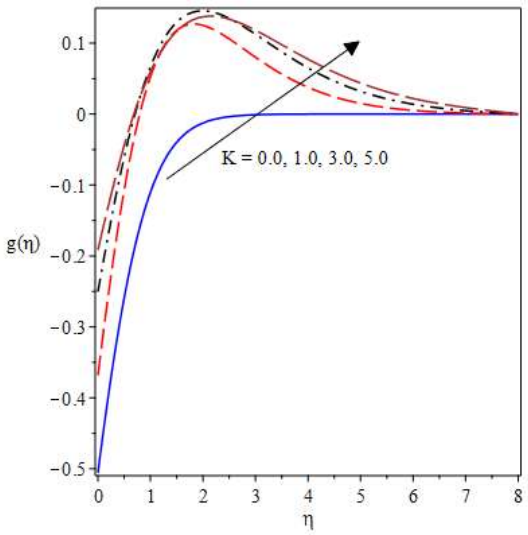

Fig. 3 Microrotation profiles for K

Figures 2 and 3 show the reactions of the velocity and microrotation profiles for various values of the material (micropolar) parameter K. It is revealed in Fig. 2 that an improvement in the magnitude of K energizes the boundary layer thickness and in consequence, the fluid flow accelerates.

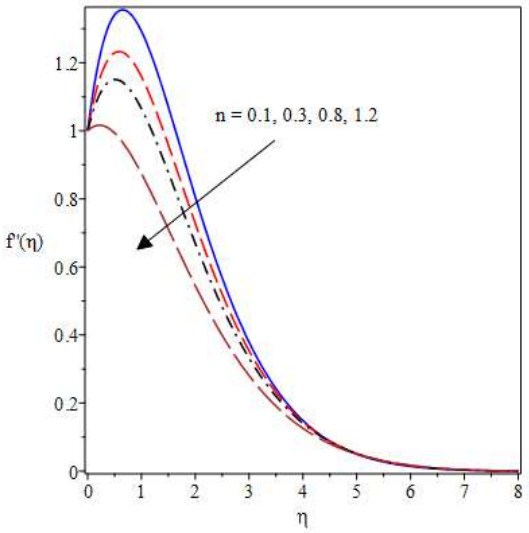

Fig. 4 Velocity field for variation of n

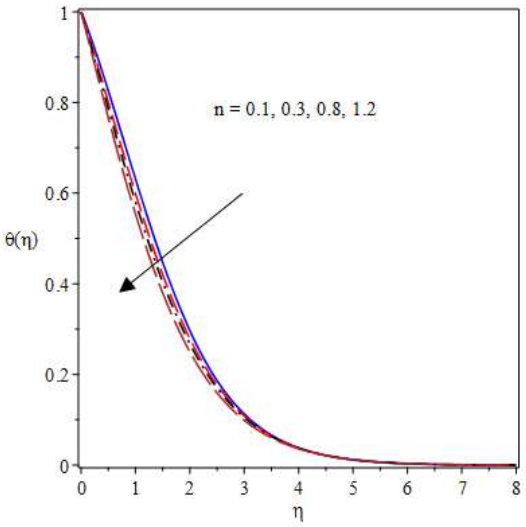

Fig. 5 Graph of temeperature for n

This response is due to a fall in the dynamic viscosity as the magnitude of material parameter K grows. From Fig. 3, an observation shows that the microrotation profile uplifts from negative to positive as K rises in magnitude. The negative values implies that there exists a reverse rotation of the micro-particles.

The graph depicting the response of velocity profiles to variation in nonlinear stretching parameter n is described in Fig. 4. One noticeable feature in this plot is that the hydrodynamic boundary layer thins out as n rises and consequently, there is a deceleration of the fluid velocity. Likewise, the thermal boundary layer falls with growth in n thereby compels a decrease in the surface temperature as the nonlinear stretching term rises as shown in Fig. 5. The plot showing the impact of the thermal Grashof number Gr on the velocity field is illustrated in Fig. 6. It is obvious that a rise in Gr enables an increase in the fluid velocity. This is due to the fact that the viscous force is reduced with a rise in the buoyancy force and as a result, the the velocity increases. Fig 7 reveals that the effect of the wall temperature parameter r is to diminish the thickness of the thermal boundary layer which then resulted into a decline in the surface temperature.

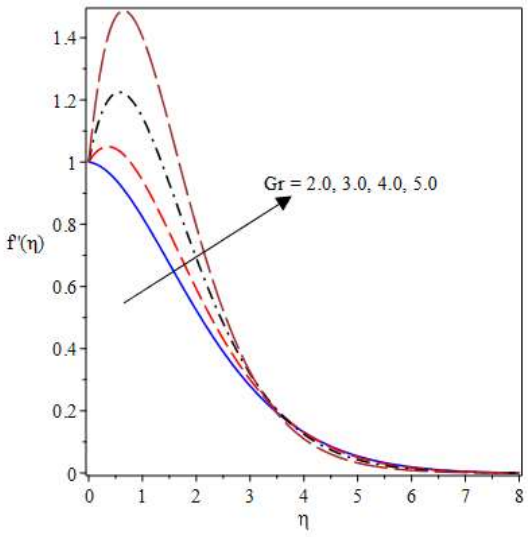

Fig. 6 The impact of Gr on velocity

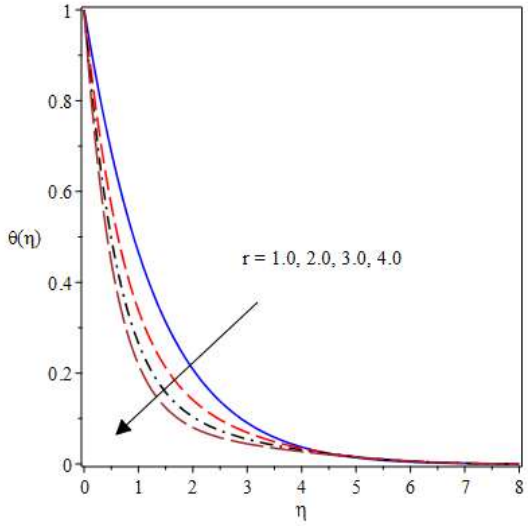

Fig. 7 Effect of r on temperature profiles

The graph of the velocity profiles versus inclination angle φ is shown in Fig. 8. Obviously, the velocity profiles decelerates with rising values of inclination angle φ, as the inclination angle rises, there is a thin hydrodynamic boundary layer. Also, it is shown that for a vertical sheet ($\varphi = 0$), a higher velocity is observed. This is so because the influence of buoyancy drops by a factor of $cos\varphi$ owing to inclination and at such, there is a reduction in the magnitude of the buoyancy driving force.

The thermal boundary layer expands and the temperature field also enlrges when the temperature-dependent heat source parameters, β uplifts as illustrated in Fig. 9. This is due to the fact that heat is being generated with increasing trend of β.

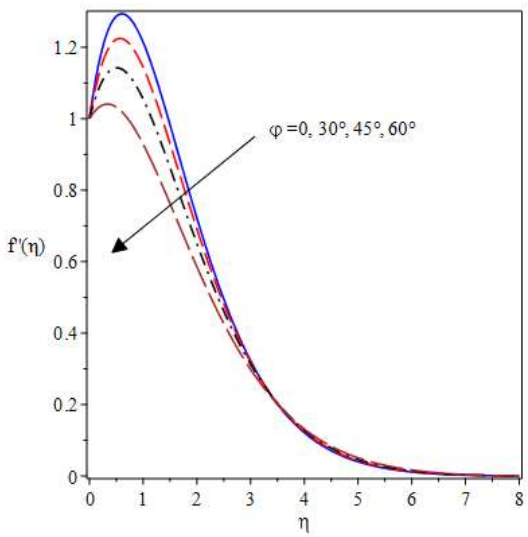

Fig. 8 Curves of velocity field versus φ

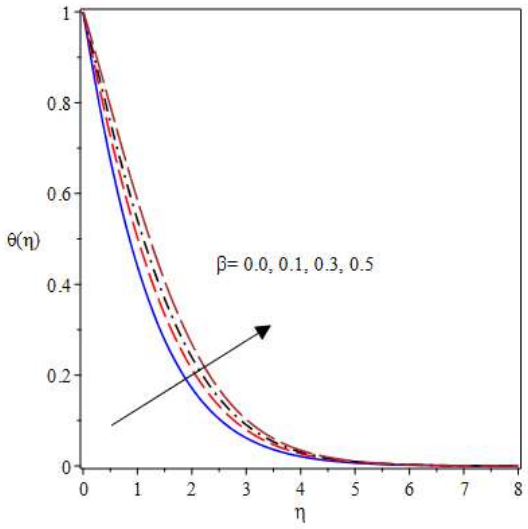

Fig. 9 Graph of temperature profiles versus β

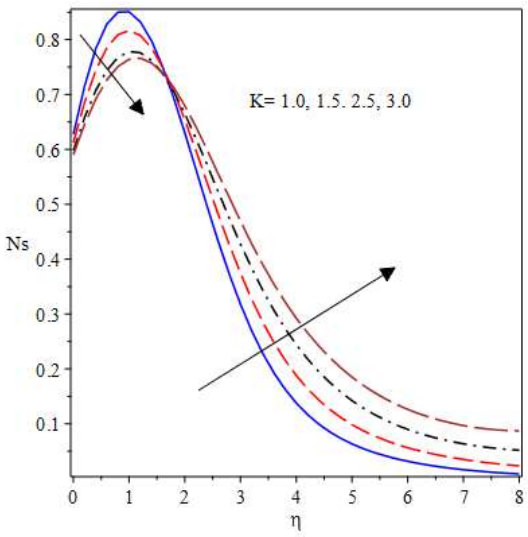

Fig. 10 Entropy number versus K

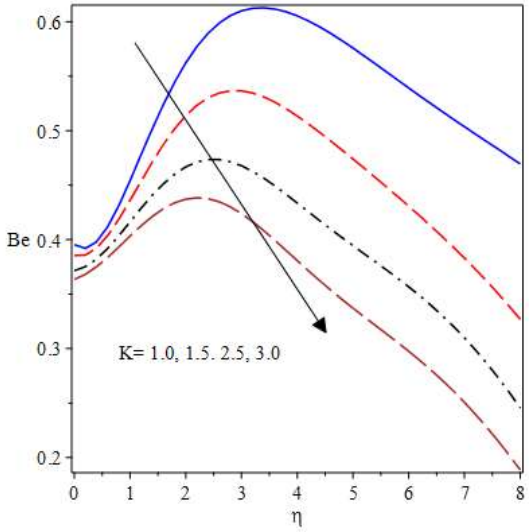

Fig. 11 Graphs of Bejan number for K

Figures 10 and 11 describe the impact of K on the profiles of entropy number and Bejan number respectively. It is clear from Fig. 10 that there is a decline in the entropy number near the wall of the stretching sheet, however, away from the sheet, there is a hike in the entropy generation as K rises. From Fig. 11, it is observed that frictional heating and magnetic field irreversibilities dominate that of heat transfer due to a decrease in the Bejan number as K improves in magnitude with increment in the value of K.

Figure 12 explains that the improvement in the radiation term Nr energizes the entropy number. More so, the Bejan number improves with a rise in the radiation term Nr. In this case, the irreversibility due to heat transfer is stronger than that of frictional and magnetic field (Ohmic heating) irreversibilities as shown in Fig. 13.

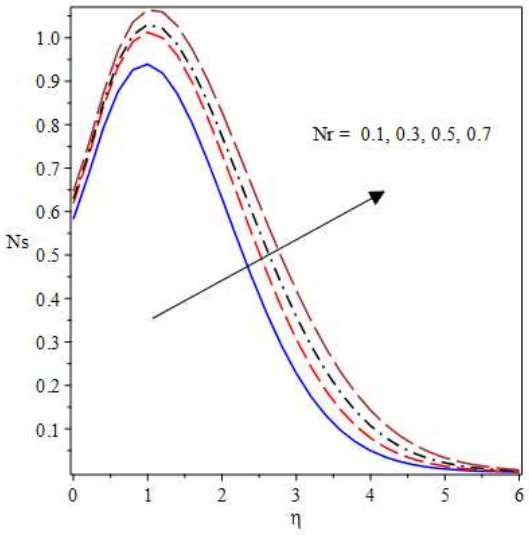

Fig. 12 Entropy generation for radiation Nr

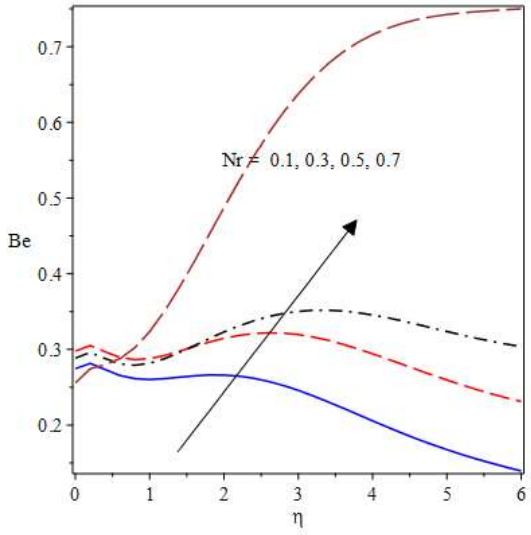

Fig. 13 Bejan number for radiation Nr term

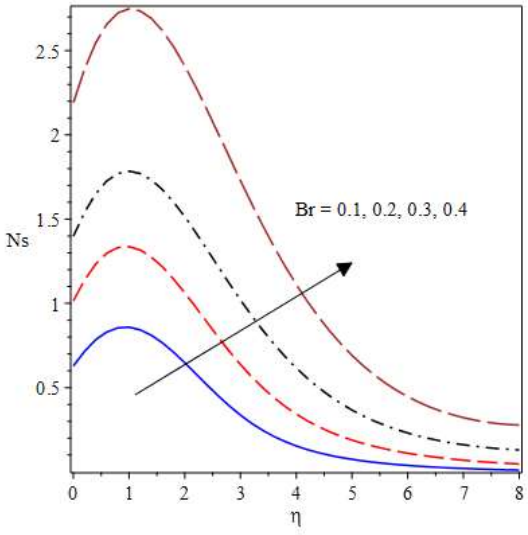

Fig. 14 Plot of entropy number versus Br

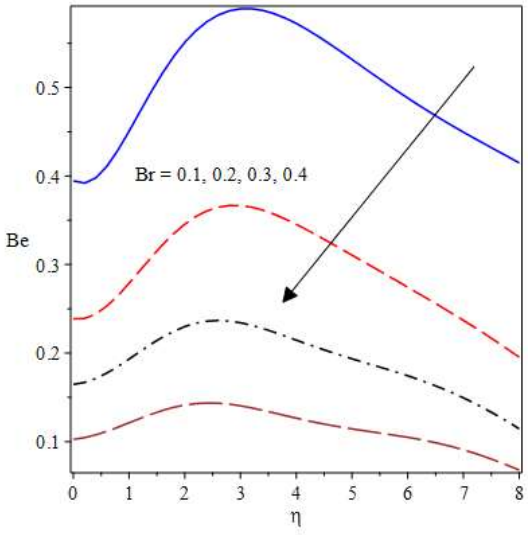

Fig. 15 Curves of Br versus Bejan number Be

The plot showing the reaction of the Brikman number Br on the entropy generation number is demonstrated in Fig. 14. Brikman number shows the product of the Eckert and Prandtl numbers, hence an increase in Br propels the entropy generation number to escalate as seen in Fig. 14. Meanwhile, an advancement in Br causes a downward trend in the Bejan number as presented in Fig. 15. In this situation, the viscous dissipation and magnetic field irreversibilities override that of heat transfer effect.

5. CONCLUSION

The investigation of irreversibility analysis of an electrically conducting micropolar fluid flow configured in an inclined permeable stretchable sheet is carried out. The influences of viscous dissipation, thermal radiation, variable viscosity, non-uniform heat source/sink and power law temperature at the boundary are also investigated on the model. The numerical solutions to the formulated governing equations are derived through the shooting technique associated with Runge-Kutta. The solutions compared favourably with the related studies in literature in the limiting situations while the influences of the main physical parameters that emerge from the model are discussed graphically. It has been found that:

- Incremental values of the radiation Nr as well as Brikman number Br parameters boost the entropy generation while the thermal boundary layer enlarges with an increas in the temperature-dependent heat source..
- An advancement in the strength of the material parameter K lowers the Bejan number and hence, empower frictional and Ohmic heating irreversibilities whereas the trend is reversed with higher values of the radiation term Nr.
- The hydrodynamic boundary layer abounds with uplift in the strength of the material term K and Grashof number Gr whereas the converse is the case for the nonlinear stretching term n and inclination angle parameter φ.

REFERENCES

1. Afridi, M. I., Qasim, M., Khan, I. and Shafie, S. and Alshomran, A. S. (2017).. Entropy generation in magnetohydrodynamic mixed convection flow over an inclined stretching sheet. *Entropy, 19*, 1-11.
2. Akinbobola, T. E. and Okoya, S.S. (2015). The flow of second grade fluid over a stretching sheet with variable thermal conductivity and viscosity in the presence of heat source/sink. *Journal of the Nigerian Mathematical Society*, 34, 331-342.
3. Al-Khaled, K, Khan, S. U. and Khan, (2020). Chemically reactive bio convection flow of tangent hyperbolic Nanoliquid with gyrotactic microorganisms and nonlinear thermal radiation, *Heliyon* 6, 1-7
4. Cortell, R, (2007). Viscous flow and heat transfer over a nonlinearly stretching sheet. *Applied Mathematics and Computation, 184*, 2007, 864-873.
5. Cortell, R. (2008). Effects of viscous dissipation and radiation on the thermal boundary layer over a nonlinearly stretching sheet. *Physics Letters A, 372*, 631-636.
6. Crane, L. J.. Flow past a stretching plate. *Communicatios Breves, 21*, 1970, 645-647.
7. Dalir, N, Dehsara, M and S. S. Nourazaret. (2014). Entropy analysis for magnetohydrodynamic flow and heat transfer of a Jeffrey nanofluid over a stretching sheet, Energy, http://dx.doi.org/10.1016/j.energy.2014.11.021
8. Das, K., Jana, S, and Kundu, P.K. (2015). Thermophoretic MHD slip flow over a permeable surface with variable fluid properties. *Alexandria Engineering Journal,* 54, 35-44.
9. Eringen, A. C. (1966).Theory of micropolar fluids. *J. Math. Anal. Appl., 16*, 1-18.
10. Eringen, A. C. (1972). Theory of thermo-microfluids. *Journal of Mathematical Analysis and Applications, 38*, 480-496.
11. Fatunmbi, E. O and Adeniyan, A. (2018). Heat and Mass Transfer in MHD Micropolar Fluid Flow over a Stretching Sheet with Velocity and Thermal Slip Conditions*, Open Journal of Fluid Dynamics,* 8, 195-215.
12. Fatunmbi, E. O. and Fenuga, O. J. (2017). MHD micropolar fluid flow over a permeable stretching sheet in the presence of variable viscosity and thermal conductivity with Soret and Dufour effects. *International Journal of Mathematical Analysis and Optimization: Theory and Applications*, 2017, 211- 232
13. Fatunmbi, E. O. and Okoya, S. S. (2020). Heat transfer in boundary layer magneto-micropolar fluids with temperature-dependent material properties over a stretching sheet, *Advances in Materials Science and Engineering,* 1-11.
14. Fatunmbi, E.O., Okoya, S. S. and Makinde, O. D. (2020). Convective heat transfer analysis of hydromagnetic micropolar fluid flow past an inclined nonlinear stretching sheet with variable thermo-physical properties. *Diffusion Foundations,* 26, 63-77..
15. Gbadeyan, J. A., Titiloye, E. O. and Adeosun, A. T. (2020). Effect of variable thermal conductivity and viscosity on Casson nanofluid flow with convective heating and velocity slip., *Heliyon* 6, 1-10.
16. Gholinia, M., Gholinia, S., Hosseinzadeh, Kh. and Ganji, D. D. (2018). Investigation on ethylene glycol nanofluid flow over a vertical permeable circular cylinder under effect of magnetic field, *Results in Physics*, 9, 1525-1533.
17. Grubka, L. J. and Bobba, K. M. (1985). Heat transfer characteristic of a continuous stretching surface with variable temperature, *Journal of Heat Transfer*, 107, 248-250.
18. Gupta, P. S. and Gupta, A. S. (1977). Heat and mass transfer on a stretching sheet with suction or blowing. *Can. J. Chem. Eng., 55*, 744-746.

19. Hayat, T., Awais, M., Asghar, S., (2013). Radiative effects in a three dimensional flow of MHD Eyring-Powell fluid. *J. Egypt Math. Soc*. 21, 379-384.
20. Hayat, T., Abbas, Z, Javed, T. (2008). Mixed convection flow of micropolar fluid over a non-linearly stretching sheet. *Physics Letters A*. 372, 637-647.
21. Ishak, A. (2010). Similarity solutions for flow and heat transfer over a permeable surface with convective boundary condition, *Applied Mathematics and Computation*, 217, 837-842.
22. Khan, I., Fatima, S., Malik, M. Y.and Salahuddin, T. (2018). Exponentially varying viscosity of magnetohydrodynamic mixed convection Eyring-Powell nanofluid flow over an inclined surface, Results in Physics, 8, 1194203.
23. Kumar, L (2013). Finite element analysis of combined heat and mass transfer in hydromagnetic micropolar flow along a stretching sheet. *Comput Mater Sci, 46*, 2009, 841-848. Doi: 10.1371/journal.pone.0059393.
24. Lu, D., Ramzan, M., Ahmadi, S. Chung, J. D., Farooq, U., A numerical treatment of MHD radiative flow of micropolar nanofluid with homogeneous-heterogeneous reactions past a nonlinear stretched surface, *Scientific Reports,* 8, 2018, 1-17.
25. Lukaszewicz, G. (1999. *Micropolar fluids: Theory and Applications* (1st Ed.). Birkhauser, Boston,
26. Makinde, O. D. and Eegunjobi, A. S. (2018). Entropy analysis in MHD flow with heat source and thermal radiation past a stretching sheet in a porous medium. {\it Defect and Diffusion Forum, 387}, 364-372.
27. Makinde, O. D. (2012). Effect of variable viscosity on thermal boundary layer over a permeable flat plate with radiation and a convective surface boundary condition. *Journal of Mechanical Science and Technology*. 26(5), 1615~1622.
28. Makinde, O. D. 2010). Similarity Solution of Hydromagnetic Heat and Mass Transfer Over a Vertical Plate with a Convective Surface Boundary Condition. *International Journal of the Physical Sciences,* 5, 700-710.
29. Mondal, H., Mondal, S., Mishra, S., Kundu, P.K and Sibanda, P. (2020). Entropy generation of variable viscosity and thermal radiation on magneto nanofluid flow with dusty fluid, *J. Appl. Comput. Mech*, 6(1), 171-182.
30. Parida, S. K., Panda, A, S., and Rout, B. R. (2015). MHD boundary layer slip flow and radiative nonlinear heat transfer over a flat plate with variable fluid properties and thermophoresis. {\it Alexandria Engineering Journal}, 54, 941-953.
31. Qasim, M., Khan, I. and Shafle, S. (2013). Heat transfer in a micropolar fluid over a stretching sheet with Newtonian heating. *Plos One, 8*(4), 1-6.
32. Reena and Rana, U. S. (2009). Effect of Dust Particles on rotating micropolar fluid heated from below saturating a porous medium. *Applications and Applied Mathematics: An International Journal. 4*, 189-217.
33. Ullah, I., Shafie, S., Khan, I., (2017). Effects of slip condition and Newtonian heating on MHD flow of Casson fluid over a nonlinearly stretching sheet saturated in a porous medium, *Journal of King Saud University Science*, 29, 250-259.